International Journal of Innovative Computing, Information and Control
Volume **20**, Number **3**, June **2024**

ICIC International ©2024 ISSN 1349-4198
pp. **725–737**

VARIABLE COUPLING CONTAINMENT CONTROL IN HETEROGENEOUS MULTI-AGENT SWITCHING TOPOLOGY BASED ON EVENT-TRIGGERED

Wenchao Ma

Department of Locomotive and Vehicle Engineering
Zhengzhou University of Railway Engineering
Sanshilipu, Jianshe West Road, Zhongyuan District, Zhengzhou 450000, P. R. China
mawenchao.99@163.com

Received August 2023; revised December 2023

Abstract. *This paper addresses the containment control problem of heterogeneous Multi-Agent Systems (MAS) under switched topology and proposes an event-triggered decoupling coefficient control strategy. Inspired by the leader-follower output regulation problem, the leaders are treated as external systems. Firstly, a distributed dynamic feedback control scheme is designed for the followers' controllers, integrating the event-triggered control mechanism. Secondly, effective coordination control rules for the variable coupling coefficients among multi-agents are devised under the switched topology condition. By comparing with the fixed coupling coefficient MAS, the designed controller not only avoids collisions among agents but also improves the convergence speed of the system. The followers can converge faster to the convex hull formed by multiple leaders. Furthermore, the event-triggered control mechanism effectively reduces the amount of information exchanged among agents, thus reducing communication load and network energy consumption. Finally, the theoretical results are validated through simulation examples.*

Keywords: Heterogeneous multi-agent systems, Event-triggered, Variable coupling, Switching topology, Containment control

1. **Introduction.** In recent years, Multi-Agent Systems (MAS) have demonstrated remarkable capabilities in addressing large and intricate problems, showcasing excellence in distribution, coordination, and autonomy [1-3]. Compared with some complex microsystems, MAS has the advantages of a simple structure and can solve complex problems by coordinating a single agent, for example, formation and attitude control of aircraft [4,5], synchronization control and tracking [6,7], and cooperative consistency control of UAVs [8,9]. The nature of these studies is to provide a class of autonomous agents to complete specific assignments through distributed control strategies. The containment control problem of MAS was first proposed by Dimarogonas et al. [30]. The essence is the consistency problem of MAS containing multiple leaders.

The research and applications of containment control are more and more extensive [10-14]. Ye et al. compared the sampling data of agent location with and without time delay [10]. Li et al. further investigated the containment control of nonlinear MAS with time delay [13]. [12] considered the distributed inclusive control problem with nonconvex control input constraints and proposed a distributed algorithm that utilizes only local information. The above researches are carried out under the premise of continuous communication, which will occupy a lot of communication resources. To solve this problem, scholars have combined the event-triggered control theory with multi-agent control [15-17]. The triggering mechanism of the Laplacian matrix independent of the communication

DOI: 10.24507/ijicic.20.03.725

graph is proposed in [16]. Xu et al. solved the problem of a multi-Euler-Lagrange system to realize event-triggered containment control in a completely distributed, buffet-free way under both static and dynamic conditions when the directed communication network does not use global information and discontinuous terms [17].

However, in many practical tasks, collision avoidance between agents must be considered, and faster convergence to a stable state within a finite time is required, such as satellite clustering, multi-rotor aircraft formation flying, and distributed scheduling [18,19]. [20] studied the collision avoidance adaptive control problem for unmanned surface vehicles. They proposed a finite-time disturbance observer to estimate and compensate for external disturbances, ensuring that all followers can enter the convex hull spanned by the leader while avoiding collisions. In [21], a combination of artificial potential field method and neural network technology was used to design a collision avoidance robust formation tracking control strategy for a class of nonlinear MAS. [22] investigated the formation control problem for a group of fixed-wing unmanned aerial vehicles under unknown disturbances. To ensure the safety of each UAV, a smooth collision avoidance potential function was designed. In addition, it is also a matter of discussion among scholars as to how to increase the speed of reaching the target state [23-25]. For example, [23] investigated the problem of steering a multi-agent system towards heterogeneous target nodes in both finite-time and fixed-time durations. In [24], a novel robust continuous-time optimization algorithm was proposed, ensuring the timely convergence of distributed problems.

In practical applications, the communication topology of multi-agent systems may undergo changes due to random factors such as sensor errors and environmental interference, rendering continuous and uninterrupted information transmission between agents infeasible. To address this challenge, we propose the integration of an event-triggered transmission mechanism within a switching topology framework. This, in conjunction with a coordinated control algorithm featuring a variable coupling coefficient, offers a viable solution for tackling the inclusion control problem in dynamic network topologies. Distinguishing itself from prior literature, which primarily focuses on collision avoidance and convergence enhancement, this paper presents an innovative variable coupling coefficient approach. This approach not only ensures collision avoidance among agents within a multi-agent system but also significantly accelerates system convergence, with a reduction of nearly 30% in convergence time. Furthermore, the utilization of event-triggered transmission control eliminates the need for continuous communication among multiple agents, leading to substantial savings in communication resource utilization. The principal contributions of this paper can be summarized as follows.

1) For an MAS with a variable coupling coefficient in switching topology, an effective coordination control rule is designed. By comparing the results with fixed coupling coefficients in an MAS, the proposed controller not only prevents collisions between agents but also enhances the convergence speed of the system. The followers can converge more rapidly within the convex hull formed by multiple leaders.

2) In designing the controllers for the followers, an event-triggered control mechanism is introduced to formulate a protocol for distributed state observers in a switching topology. This enables the agents that cannot directly obtain information from the leaders to estimate the leaders' states. The switching topology imposes less communication constraint on the system.

3) An event-triggered control mechanism is designed to reduce the communication within MAS and the number of controller updates. This significantly decreases energy consumption and demonstrates that the proposed control strategy effectively eliminates Zeno behavior.

Notations: N denotes the set of positive integers. $\boldsymbol{R}^n$ represents the vector space on the n-dimensional entity $\boldsymbol{R}$, and $\boldsymbol{R}^{n\times n}$ represents the dimensional real matrix space. $\boldsymbol{P}\otimes\boldsymbol{Q}$ is the Kronecker product of matrices $\boldsymbol{P}$ and $\boldsymbol{Q}$. $diag\{\Theta_1,\Theta_2,\ldots,\Theta_n\}$ represents the diagonal matrix with elements Θ_i, $i=1,2,\ldots,n$. $\mathbf{1}_n$ is an n-dimensional column vector with all ones. I_n is an n-dimensional square matrix whose elements on the main diagonal are all 1 and the rest are all 0. $\mathbf{0}$ represents all zero matrices, $\boldsymbol{A}>0$ denotes $\boldsymbol{A}$ symmetric positive definite matrix, and Λ^T is the transpose of matrix Λ.

The remaining components of this article are as follows: Section 2 introduces the mathematic preliminaries; Section 3 describes the system control scheme design; the main results are given in Section 4; in Section 5, experimental simulations are carried out to prove the correctness of the theory; the last section draws conclusions.

2. Mathematic Preliminaries.

2.1. Basic theory of communication topographies.

The topology of information interaction between agents is denoted by $G=\{\boldsymbol{V},\varepsilon,\boldsymbol{A}\}$, where $\boldsymbol{V}=\{1,2,\ldots,N\}$ represents the set of vertices of N agents, and every agent acts as a vertex of the weighted graph $G=\{\boldsymbol{V},\varepsilon,\boldsymbol{A}\}$. $\varepsilon\in\{\boldsymbol{V}*\boldsymbol{V}\}$ denotes the set of agents where communication exists between them. $\boldsymbol{A}=(a_{ij})\in\boldsymbol{R}^{n\times n}$ denote the neighbor matrix of graph G, and i, j denote different agents. The neighbors of the ith agent can be denoted by $N_i=\{j\in\boldsymbol{V}:(i,j)\in\varepsilon, i\neq j\}$. Suppose there is no loop of its own nodes in the graph, i.e., $(i,i)\notin\varepsilon$, if $(i,j)\in\varepsilon$, then $a_{ij}>0$, which means that point j is an adjacent node of point i, otherwise $a_{ij}=0$. If $(i,j)\in\varepsilon$ and $(j,i)\in\varepsilon$, then the graph G is known as an undirected graph, otherwise it is a directed graph.

The information interaction topology graph G is composed of followers and leaders, which is a disconnected graph under the condition of switching topology. $d_{in}(v_n)=\sum_{i=1}^{n}a_{ij}$ is the in-degree of node i, and define the in-degree matrix of graph G as $D_{in}=diag\{d_{in}(v_1),\ldots,d_{in}(v_n)\}$, and the Laplacian matrix as

$$l_{ij}=\begin{cases}-a_{ij}, & i\neq j\\ \sum_{i=1}^{n}a_{ij}, & i=j\end{cases}. \tag{1}$$

2.2. Relevant definitions and lemmas.

Definition 2.1. [26] *$\wp$ is a collection of real vector spaces $\boldsymbol{W}\subseteq\boldsymbol{R}^n$. If there is a point $(1-z)x+zy\in\wp$ for random z $(0\le z<1)$ and random x, y in the set $\wp$, then $\wp$ is said to be convex. The convex hull of point set $X=\{x_1,x_2,\ldots,x_n\}$ in $\boldsymbol{W}$ is the minimize convex set containing all points in X, and expressed by* $\mathrm{Co}(X)$, *then*

$$\mathrm{Co}(X)=\left\{\sum_{i=1}^{n}\alpha_i x_i\,\middle|\, x_i\in X,\alpha_i\in\boldsymbol{R},\alpha_i\ge 0,\sum_{i=1}^{n}\alpha_i=1\right\}. \tag{2}$$

Definition 2.2. *Consider a containment control MAS with multiple leaders composed of $p+q$ agents, including p followers and q leaders, and define the subscript set of followers as $F=\{1,2,\ldots,p\}$, the leaders as $\boldsymbol{R}=\{p+1,p+2,\ldots,p+q\}$. Since the entry of the leader is zero and considering the dynamic switching topology of MAS, the Laplacian matrix of G can be written as follows:*

$$\mathcal{L}^{\xi_t}=\begin{bmatrix}\mathcal{L}_{FF}^{\xi_t} & \mathcal{L}_{LF}^{\xi_t}\\ \mathbf{0} & \mathbf{0}\end{bmatrix}, \tag{3}$$

where $\mathcal{L}_{FF}^{\xi_t} \in \boldsymbol{R}^{n\times n}$, $\mathcal{L}_{LF}^{\xi_t} \in \boldsymbol{R}^{n\times m}$, ξ_t *is the switch signals of the system communication topology.*

Definition 2.3. [27] *If the control law designed for each follower can ensure that they all converge to the convex hull crossed by the dynamic leader, then it is said that the agents with multiple leaders realize the bounding control, i.e.,*

$$\lim_{t\to\infty} dis\{x_i(t), conv\{x_j(t)|i \in F, j \in \boldsymbol{R}\}\} = 0. \tag{4}$$

Assumption 2.1. *Consider a set of nonempty, bounded and continuous time intervals* $[t_k, t_{k+1})$, $k = 0, 1, \ldots, n$, *where* $t_0 = 0$, $t_{k+1} - t_k \le \delta_1$, $\delta_1 > 0$. *There exists a finite number of time subintervals* $\left[t_k^r, t_k^{r+1}\right)$, $r = 0, 1, \ldots, m_k - 1$, $t_k^0 = t_k$, $t_k^{m_k} = t_{k+1}$, $m_k \ge 0$, *in the time interval* $[t_k, t_{k+1})$, $k = 0, 1, \ldots, n$, *and* $t_k^{r+1} - t_k^r \ge \delta_2$, $\delta_2 > 0$.

Assumption 2.2. *When* $t \in [0, +\infty)$ *has* $\xi_t \in \aleph$, $\aleph = \{1, 2, \ldots, \phi\}$, G_{ξ_t} *represents the topology of the MAS at time t, and its Laplace matrix is represented by* $\mathcal{L}^{\xi_t}$, ϕ *is the total number of switching signals.*

Assumption 2.3. *The communication topology* G_{ξ_t} *of MAS switches at time* t_k, *so its topology keeps constant during interval* $[t_k, t_{k+1})$. *For followers in the communication topology, at least one leader communicates with the follower.*

Lemma 2.1. [28] *According to Assumption 2.3,* $\mathcal{L}_{FF}$*'s eigenvalues have positive real parts,* $-\mathcal{L}_{FF}^{-1}\mathcal{L}_{RF}$*'s elements are nonnegative, and the sum of every row element of matrix* $-\mathcal{L}_{FF}^{-1}\mathcal{L}_{RF}$ *is one.*

Assumption 2.4. *The matrix* $(\boldsymbol{A}_i, \boldsymbol{B}_i)$ *is stable.*

Assumption 2.5. *The eigenvalues of the matrix* $\boldsymbol{A}$ *are nonnegative.*

Assumption 2.6. *The linear matrix equation*

$$S = \boldsymbol{A}_i + \boldsymbol{B}_i U_i, \quad i \in F, \tag{5}$$

has solutions U_i.

3. System Control Scheme Design.

The system description is as follows:

$$\begin{cases} \dot{x}_i(t) = \boldsymbol{A}_i x_i(t) + \boldsymbol{B}_i u_i(t), & t \ge 0,\ i \in F, \\ \dot{v}_k(t) = S v_k(t), & t \ge 0,\ i \in \boldsymbol{R}, \end{cases} \tag{6}$$

where $x_i(t) \subseteq \boldsymbol{R}^n$ and $u_i(t) \subseteq \boldsymbol{R}^p$ are the state and control input of the ith follower respectively, and $\boldsymbol{A}_i \in \boldsymbol{R}^{n\times n}$, $\boldsymbol{B}_i \in \boldsymbol{R}^{n\times m}$ are constant matrices of appropriate dimensions. $v_k(t) \in \boldsymbol{R}^n$ denotes the kth leading agent's state.

Define the error vector of the follower as

$$e_i(t) = \sum_{j\in N_i} a_{ij}(x_i(t) - x_j(t)) + \sum_{k=n+1}^{n+m} b_{k,i}(v_k(t) - x_i(t)), \quad i \in F, \tag{7}$$

i.e.,

$$e(t) = (\mathcal{L}_{FF} \otimes I_n)x + (\mathcal{L}_{RF} \otimes I_n)v_k, \tag{8}$$

where $e = (e_1, \ldots, e_n)^T$, $v_k = (v_{n+1}, \ldots, v_{n+m})^T$, $x = (x_1, \ldots, x_n)^T$.

3.1. Design of coordinated control law with state observer.

In practical applications, only part of the intelligence can get the signal of the external system, while the other part cannot directly get the state of the external system, so it is necessary to estimate the state of the external system. As some followers in the MAS cannot obtain theinformation of the leader, the leader's state needs the observer to evaluate so that the following agent can track leading agents and the ith follower's distributed state feedback control protocol within a certain time, as shown below [29]:

$$\begin{cases} u_i(t) = K_{i,1}x_i(t) + K_{i,2}\boldsymbol{\eta}_i(t), \\ \dot{\boldsymbol{\eta}}_i(t) = S\boldsymbol{\eta}_i(t) + \gamma \left[\sum_{j\in N_i} - a_{ij}(\boldsymbol{\eta}_i(t) - \boldsymbol{\eta}_j(t)) + \sum_{k=n+1}^{n+m} b_{k,i}(v_k(t) - \boldsymbol{\eta}_i(t)) \right], \end{cases} \tag{9}$$

where $K_{i,1}, K_{i,2} \in \boldsymbol{R}^{p\times N}$ are controller gain matrices. $\gamma > 0$, $\boldsymbol{\eta}_i(t) \in \boldsymbol{R}^N$ is the state of the observer. If there is no coupling relationship between multiple agents, $a_{ij} = 0$; otherwise

$$a_{ij} = \begin{cases} 0, & (x_i - x_j) < -\hat{\beta} \\ \dfrac{\hat{\beta} - |x_i - x_j|}{\gamma_1}, & \hat{\beta} - \gamma_1 < (x_i - x_j) \le \hat{\beta} \\ \dfrac{2\gamma_2\zeta - \gamma_2^2}{\zeta^2 - (x_i - x_j)^2}, & \zeta - \gamma_2 < (x_i - x_j) \le \zeta \\ 1, & \text{else} \end{cases}, \tag{10}$$

where $\hat{\beta}$ and ζ are normal numbers, $\gamma_1 \in \left(0, \hat{\beta}\right)$, $\gamma_2 \in (0, \zeta)$. $b_{k,i}$ is the weighting between the agent and the leader. If the follower establishes communication with a leader directly, then $b_{k,i} = a_{ij}$; otherwise, it is 0.

Based on the control protocol (9), the event trigger control rules are combined. $\left\{k_{w_i}^i\right\}$, $i \in F$ is defined as the triggering moment of the ith event of the w_ith follower, and let $\hat{\boldsymbol{\eta}}_i(t) = \boldsymbol{\eta}_i\left(k_{w_i}^i\right)$ represent the marking data of the ith event follower state triggering moment. Protocol (9) can be rewritten as

$$\begin{cases} u_i(t) = K_{i,1}x_i(t) + K_{i,2}\hat{\boldsymbol{\eta}}_i(t), \\ \dot{\hat{\boldsymbol{\eta}}}_i(t) = S\hat{\boldsymbol{\eta}}_i(t) + \gamma \left[\sum_{j\in N_i} - a_{ij}(\hat{\boldsymbol{\eta}}_i(t) - \hat{\boldsymbol{\eta}}_j(t)) + \sum_{k=n+1}^{n+m} b_{k,i}\left(v_k(t) - \hat{\boldsymbol{\eta}}_i(t)\right) \right]. \end{cases} \tag{11}$$

The system (6), containment error (7) and control law (11) are expressed as

$$\begin{cases} \dot{x}_c(t) = \boldsymbol{A}_c x_c(t) + \boldsymbol{B}_c \bar{v}_k(t), \\ \dot{\bar{v}}_k(t) = \bar{S}\bar{v}(t), \\ e(t) = D_c x_c(t) + E_c \bar{v}_k(t), \\ \dot{\hat{\boldsymbol{\eta}}}_i(t) = S\hat{\boldsymbol{\eta}}_i(t) + \gamma \left[\sum_{j\in N_i} - a_{ij}(\hat{\boldsymbol{\eta}}_i(t) - \hat{\boldsymbol{\eta}}_j(t)) + \sum_{k=n+1}^{n+m} b_{k,i}(v_k(t) - \hat{\boldsymbol{\eta}}_i(t)) \right], \end{cases} \tag{12}$$

where $x_c(t) = \left[x_i(t)^T, \boldsymbol{\eta}_i(t)^T\right]^T$ is the state of the closed loop system, $\bar{v}_k(t) = \mathbf{1}_n \otimes v_k(t)$, $\bar{S} = I_n \otimes S$, $\boldsymbol{A}_c = \begin{bmatrix} \boldsymbol{A} + \boldsymbol{B}K_1 & \boldsymbol{B}K_2 \\ 0 & \bar{S} - \boldsymbol{\mathcal{L}}_{FF} \otimes \gamma \end{bmatrix}$, $\boldsymbol{B}_c = \begin{bmatrix} 0 \\ -\boldsymbol{\mathcal{L}}_{RF} \otimes \gamma \end{bmatrix}$, $D_c = \begin{bmatrix} \boldsymbol{\mathcal{L}}_{FF} \otimes I_n & 0 \end{bmatrix}$, $E_c = \boldsymbol{\mathcal{L}}_{RF} \otimes I_n$.

Definition 3.1. *By the control law (11), the MAS (12) will satisfy both the following requirements:*

1) The matrix $\boldsymbol{A}_c$ is Hurwitz, and $\boldsymbol{A}_c$'s eigenvalues have negative real parts;

2) For any initial situations $x_c(0)$ and $v_k(0)$,

$$\lim_{t\to\infty} e(t) = \lim_{t\to\infty} D_c x_c(t) + E_c \bar{v}_k(t) = 0. \tag{13}$$

Based on Assumption 2.4, choosing K_i^1, $i \in F$ to make $\boldsymbol{A}_i + \boldsymbol{B}_i K_i^1$ has Hurwitz stability. And there is

$$K_i^2 = U_i - K_i^1, \quad i \in F. \tag{14}$$

The solution to U_i can be derived from (5), according to (14)

$$\bar{S} = \boldsymbol{A} + \boldsymbol{B}K_1 + \boldsymbol{B}K_2, \tag{15}$$

where $\boldsymbol{A} = diag\{\boldsymbol{A}_1, \boldsymbol{A}_2, \ldots, \boldsymbol{A}_n\}$, $\boldsymbol{B} = diag\{\boldsymbol{B}_1, \boldsymbol{B}_2, \ldots, \boldsymbol{B}_n\}$, $K_1 = diag\{K_1^1, K_2^1, \ldots, K_n^1\}$, $K_2 = diag\{K_1^2, K_2^2, \ldots, K_n^2\}$, $\bar{S} = I_n \otimes S$.

3.2. **Design of event-triggered rules.** Design a distributed event-triggered algorithm for following multiple agents:

$$\|\Xi_i\| > \frac{\alpha\zeta}{\mu\beta}\|Z_i\|, \tag{16}$$

where $0 \le \sigma < 1$, $I_{n+m} \otimes \gamma = \mu$, $\zeta = \min\{\lambda_1, \ldots, \lambda_i, \ldots, \lambda_n\}$, λ_i is the eigenvalue of the matrix L, $Z = (Z_1, \ldots, Z_n)^T$, $\Xi = (\Xi_1, \ldots, \Xi_n)^T$, $\beta = \|(\mathcal{L}_1 \otimes I_{n+m})^2\|$, its state is defined as

$$Z_i = \sum_{j \in N_i} -a_{ij}(x_i(t) - x_j(t)) + \sum_{k=n+1}^{n+m} b_{k,i}(v_k(t) - x_i(t)), \quad i \in F. \tag{17}$$

The state error vector is

$$\Xi_i = \sum_{j \in N_i} -a_{ij}\left(\hat{x}_i(t) - \hat{x}_j(t)\right) + \sum_{k=n+1}^{n+m} b_{k,i}\left(v_k(t) - \hat{x}_i(t)\right) - Z_i. \tag{18}$$

In the designed event-triggering algorithm, when the condition of event-triggering is met, the follower updates their information at the trigger time $\left\{k_{w_i}^i\right\}$, $i \in F$, and there is no information exchange between agents between the two trigger intervals.

4. Main Result.

Theorem 4.1. *For the system (12), by Definition 3.1, if there is a constant matrix X_c meeting the equation*

$$X_c\bar{S} = \boldsymbol{A}_c X_c \boldsymbol{B}_c, \quad 0 = D_c X_c + E_c. \tag{19}$$

Then $\lim_{t\to\infty} e(t) = 0$. According to Assumptions 2.4-2.6 and Definition 3.1, the MAS (6) can realize containment control when $\lim_{t\to\infty} e(t) = 0$, i.e., $\lim_{t\to\infty} x = \left(-\mathcal{L}_{FF}^{-1}\mathcal{L}_{RF} \otimes I_n\right) v$.

Proof: Let

$$\hat{x}_c(t) = x_c(t) - X_c \sum_{k=n+1}^{n+m} \bar{v}_k(t). \tag{20}$$

According to (19),

$$\begin{aligned}
\dot{\hat{x}}_c(t) &= \dot{x}_c(t) - X_c \sum_{k=n+1}^{n+m} \dot{\bar{v}}_k(t) \\
&= \boldsymbol{A}_c x_c + \sum_{k=n+1}^{n+m} \boldsymbol{B}_c \bar{v}_k(t) - X_c \sum_{k=n+1}^{n+m} \bar{S}\bar{v}_k(t) \\
&= \boldsymbol{A}_c x_c(t) + \sum_{k=n+1}^{n+m} \boldsymbol{B}_c \bar{v}_k(t) - \left(\sum_{k=n+1}^{n+m} \boldsymbol{A}_c X_c \bar{v}_k(t) + \sum_{k=n+1}^{n+m} \boldsymbol{B}_c \bar{v}_k(t)\right) \\
&= \boldsymbol{A}_c x_c(t) - \boldsymbol{A}_c X_c \sum_{k=n+1}^{n+m} \bar{v}_k(t)
\end{aligned}$$

$$= \boldsymbol{A}_c\hat{x}_c(t). \tag{21}$$

Because $\boldsymbol{A}_c$ has Hurwitz stability, $\lim_{t\to\infty}\hat{x}_c(t) = 0$, according to (19),

$$\begin{aligned} e(t) &= D_c x_c(t) - \sum_{k=n+1}^{n+m} E_c\bar{v}_k(t) \\ &= D_c\hat{x}_c(t) + D_c X_c \sum_{k=n+1}^{n+m} \bar{v}_k(t) + \sum_{k=n+1}^{n+m} E_c\bar{v}_k(t) \\ &= D_c\hat{x}_c(t) + \sum_{k=n+1}^{n+m} (D_c X_c + E_c)\bar{v}_k(t). \end{aligned} \tag{22}$$

Because $0 = D_c X_c + E_c$, $e(t) = D_c\hat{x}_c(t)$, $\lim_{t\to\infty} e(t) = \lim_{t\to\infty} D_c\hat{x}_c(t) = 0$.

$$\begin{aligned} x(t) &= \left[\sum_{q=n+1}^{n+m} (\mathcal{L}_{FF}\otimes I_n)\right]^{-1} \sum_{k=n+1}^{n+m} [(\mathcal{L}_{RF}\otimes I_n)[\mathbf{1}_n\otimes v(t)]] \\ &= \sum_{k=n+1}^{n+m}\left[\left[\left(\sum_{q=n+1}^{n+m}\mathcal{L}_{FF}\right)^{-1}\otimes I_n\right](\mathcal{L}_{RF}\otimes I_n)[\mathbf{1}_n\otimes v(t)]\right], \end{aligned} \tag{23}$$

then,

$$x(t) = \sum_{k=n+1}^{n+m}\left[\left[\left(\sum_{q=n+1}^{n+m}\mathcal{L}_{FF}\right)^{-1}\mathcal{L}_{RF}\mathbf{1}_n\right]\otimes v(t)\right]. \tag{24}$$

According to Lemma 2.1,

$$\sum_{k=n+1}^{n+m}\left[\left(\sum_{q=n+1}^{n+m}\mathcal{L}_{FF}\right)^{-1}\mathcal{L}_{RF}\mathbf{1}_n\right] = \left(\sum_{q=n+1}^{n+m}\mathcal{L}_{FF}\right)^{-1}\left(\sum_{k=n+1}^{n+m}\mathcal{L}_{RF}\mathbf{1}_n\right) = \mathbf{1}_n. \tag{25}$$

When $\lim_{t\to\infty} e(t) = 0$, according to Definition 2.1 and Definition 2.3, the follower can enter the convex hull formed by the leader. $\lim_{t\to\infty} x = \left(-\mathcal{L}_{FF}^{-1}\mathcal{L}_{RF}\otimes I_n\right)v$. □

Theorem 4.2. *For heterogeneous linear MAS (6) and the protocol (11), assume that all the assumptions and conditions in Theorem 4.1 are true. According to trigger condition (16), for any initial condition, the lower limit of event trigger interval* $\left[k^i_{w_{i+1}} - k^i_{w_i}\right)$ *is* $\tau > 0$*, which is given by the following:*

$$\begin{aligned} \tau &= \frac{\alpha\zeta}{\mu\boldsymbol{\eta}(\|(I_n\otimes S)\| + \|(\mathcal{L}_{FF}\otimes\mu)\|) + \alpha\zeta\|(\mathcal{L}_{FF}\otimes\mu)\|} \\ t^i_{k+1} &- t^i_k \geq \tau, \quad k\in\{1,2,\ldots\}. \end{aligned} \tag{26}$$

Proof: Let $l = \boldsymbol{\eta} - \left(-\mathcal{L}_{FF}^{-1}\mathcal{L}_{RF}\otimes I_n\right)v$,

$$\begin{aligned} i &= (I_n\otimes S)\boldsymbol{\eta} - (\mathcal{L}_{FF}\otimes\gamma)\boldsymbol{\eta} - (\mathcal{L}_{RF}\otimes\gamma)v + (I_n\otimes\gamma)\Xi + \left(\mathcal{L}_{FF}^{-1}\mathcal{L}_{RF}\otimes S\right)v \\ &= ((I_n\otimes S) - (\mathcal{L}_{FF}\otimes\gamma))l + (I_n\otimes\gamma)\Xi, \end{aligned} \tag{27}$$

according to (16)-(18) and (27),

$$\begin{aligned} \frac{\mathrm{d}\|\Xi\|}{\mathrm{d}t} &= \frac{\Xi^T\dot{\Xi}}{\|\Xi\|} \\ &\leq \left\|-\dot{Z}\right\| \end{aligned}$$

$$
\begin{aligned}
&= \|(\mathcal{L}_{FF} \otimes I_n)\dot{\boldsymbol{\eta}} + (\mathcal{L}_{LF} \otimes I_n)\dot{v}\| \\
&= \|(\mathcal{L}_{FF} \otimes I_n)i\| \\
&= \|(\mathcal{L}_{FF} \otimes I_n)(((I_n \otimes S) - (\mathcal{L}_{FF} \otimes \gamma))l + (I_n \otimes \gamma)\Xi)\| \\
&\leq ((I_n \otimes S) + (\mathcal{L}_{FF} \otimes \mu))\|Z\| + (\mathcal{L}_{FF} \otimes \mu)\|\Xi\| \\
&\leq \left((I_n \otimes S) + (\mathcal{L}_1 \otimes \mu) + \frac{\alpha\zeta}{\mu\boldsymbol{\eta}}(\mathcal{L}_1 \otimes \mu)\right)\|Z\|, \quad t \in \left[k^i_{w_i}, k^i_{w_{i+1}}\right)
\end{aligned} \tag{28}
$$

therefore,

$$
\begin{aligned}
\tau_k &= k^i_{w_{i+1}} - k^i_{w_i} \\
&\geq \frac{\frac{\alpha\zeta}{\mu\boldsymbol{\eta}}\|Z\|}{\left((I_n \otimes S) + (\mathcal{L}_{FF} \otimes \mu) + \frac{\alpha\zeta}{\mu\boldsymbol{\eta}}(\mathcal{L}_{FF} \otimes \mu)\right)\|Z\|}, \\
&= \frac{\alpha\zeta}{\mu\boldsymbol{\eta}((I_n \otimes S) + (\mathcal{L}_{FF} \otimes \mu)) + \alpha\zeta(\mathcal{L}_{FF} \otimes \mu)} \\
&> 0.
\end{aligned} \tag{29}
$$

So, the lower limit τ of event-triggered interval $\left\{k^i_{w_{i+1}} - k^i_{w_i}\right\}$ is larger than 0, and Zeno behavior is excluded. □

5. **Simulation Example.** On the basis of theoretical analysis, a simulation example is given to verify the results. From Figure 1, 1, 2, 3, and 4 are the following agents, and 5, 6, and 7 are the leading agents. The design of the topology diagram in this study considers the necessity of a directed topology to possess a spanning tree connecting the followers. Furthermore, it requires the leader to maintain a communication link with at least one follower, independent of the communication between the leaders. Three unique topology diagrams, depicted in Figure 1, were formulated, and simulations were executed to authenticate the approach outlined in this research.

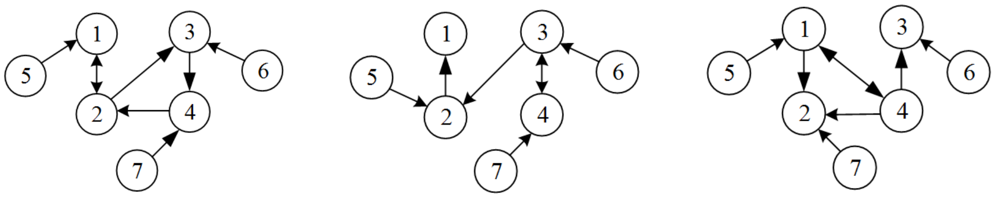

FIGURE 1. The communication topology of MAS

According to the simulation experiment, the corresponding dynamic equation matrix of system (6) is given as $S = \begin{bmatrix} 1 & -3 \\ 1 & -1 \end{bmatrix}$, $\boldsymbol{A}_1 = \begin{bmatrix} 1 & -1 \\ 1 & 0 \end{bmatrix}$, $\boldsymbol{B}_1 = \begin{bmatrix} -2 \\ -1 \end{bmatrix}$, $\boldsymbol{A}_2 = \begin{bmatrix} 2 & 0 \\ 2 & 2 \end{bmatrix}$, $\boldsymbol{B}_2 = \begin{bmatrix} -1 \\ -1 \end{bmatrix}$, $\boldsymbol{A}_3 = \begin{bmatrix} 2 & -1 \\ 3 & 3 \end{bmatrix}$, $\boldsymbol{B}_3 = \begin{bmatrix} 1 \\ 2 \end{bmatrix}$, $\boldsymbol{A}_4 = \begin{bmatrix} -1 & -4 \\ 3 & 0 \end{bmatrix}$, $\boldsymbol{B}_4 = \begin{bmatrix} -1 \\ 1 \end{bmatrix}$. Knowing the above matrix, according to Equation (5), we can get $U_1 = \begin{bmatrix} 0 & 1 \end{bmatrix}$, $U_2 = \begin{bmatrix} 1 & 3 \end{bmatrix}$, $U_3 = \begin{bmatrix} -1 & -2 \end{bmatrix}$, $U_4 = \begin{bmatrix} -2 & -1 \end{bmatrix}$. The values of $K_{i,1}$ given in our simulations are $K_{1,1} = \begin{bmatrix} 1 & 1 \end{bmatrix}$, $K_{2,1} = \begin{bmatrix} -0.5 & 9 \end{bmatrix}$, $K_{3,1} = \begin{bmatrix} 2 & -5 \end{bmatrix}$, $K_{4,1} = \begin{bmatrix} 2 & 0 \end{bmatrix}$, from Equation (14), we get $K_{1,2} = \begin{bmatrix} -1 & 0 \end{bmatrix}$, $K_{2,2} = \begin{bmatrix} 1.5 & -6 \end{bmatrix}$.

From Figure 1, the possible information interaction topologies of the MAS are $\{G_1, G_2, G_3\}$. The topology is switched in order of preference $G_1 \to G_2 \to G_3 \to G_1 \to \cdots$.

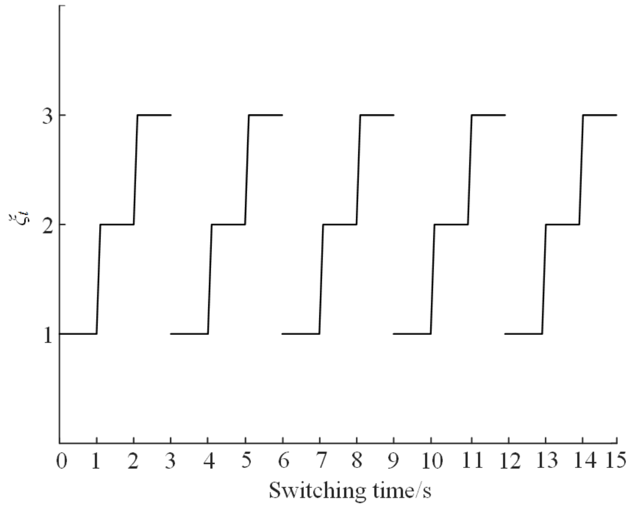

FIGURE 2. Process of switching topologies

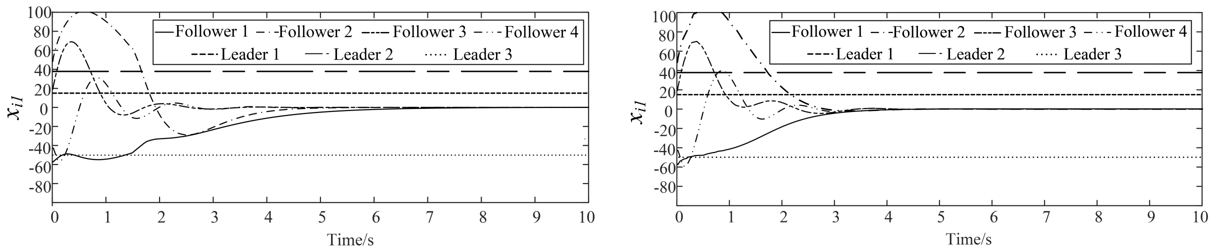

(a) (b)

FIGURE 3. State trajectories $x_{i1}(t)$ of multi-agent: (a) Before improvement; (b) after improvement

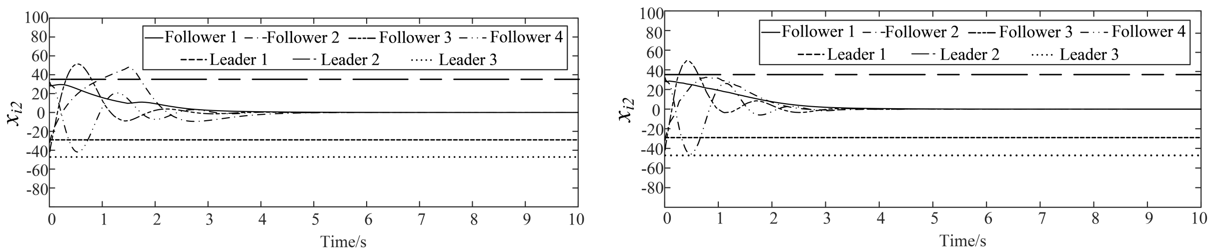

(a) (b)

FIGURE 4. State trajectories $x_{i2}(t)$ of multi-agent: (a) Before improvement; (b) after improvement

The topology switching process is shown in Figure 2. As can be seen from the figure, the residence time of each state is set to 1 s, so as to switch in the set order. Under the setup conditions of the above simulation experiment, we obtained the simulation results into the following.

In Figure 3 and Figure 4, we compare the performance of this paper proposed method with the containment control method of MAS using a fixed coupling coefficient. The state trajectory diagrams of $x_{i1}(t)$ and $x_{i2}(t)$ under the two control modes are depicted. A notable improvement can be observed. Specifically, the time for x_{i1} to reach a steady state is shortened from about 7 s to 5 s, and the convergence rate is increased by 28.5%. The steady-state time of x_{i2} is shortened from 5 s to 3.5 s, and the convergence rate is increased by 30%.

Moreover, when comparing the states of Follower 1 and Follower 2 between the two methodologies within the state trajectory x_{i1}, it becomes evident that the enhanced Followers 1 and 2, exhibit more consistent and less fluctuating state changes, reflecting superior control performance. Conversely, the state changes for Followers 3 and 4 remain less pronounced. This observation holds true for the state trajectory x_{i2} as well.

Figure 5 and Figure 6 show the state error diagrams of the observed value and the actual value of the follower $x_{i1}(t)$, $x_{i2}(t)$ under two control modes, respectively. Under the proposed method, the convergence time of the observed value and the actual value of x_{i1}'s state observer to zero is shortened from about 6 s to 4.5 s, and the convergence rate is increased by about 25%. The convergence time between the observed value and the actual value of x_{i2}'s state observer to zero is shortened from about 5 s to 4 s, and the convergence speed is increased by about 20%. Similar to the state trajectory, the error variation of the improved system e_{i1} and e_{i2} fluctuates less and changes more smoothly. Figure 7 shows the trigger moments of the following agents, which reduces the number of communication and controller updates within MAS, reduces energy consumption, and can also verify that Zeno behavior will not appear in the system.

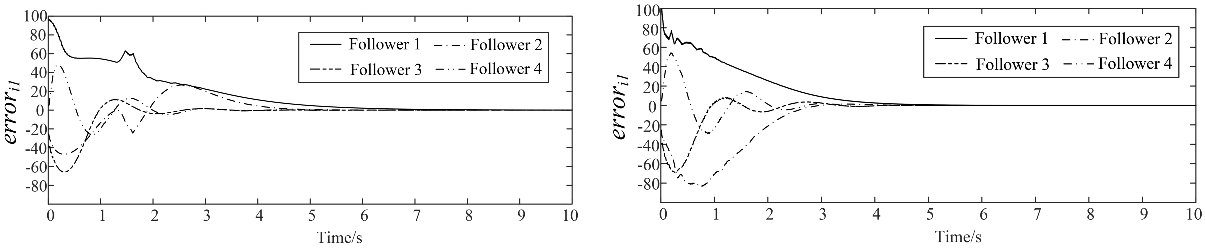

(a) (b)

FIGURE 5. $e_{i1}(t)$ between the observed and actual values: (a) Before improvement; (b) after improvement

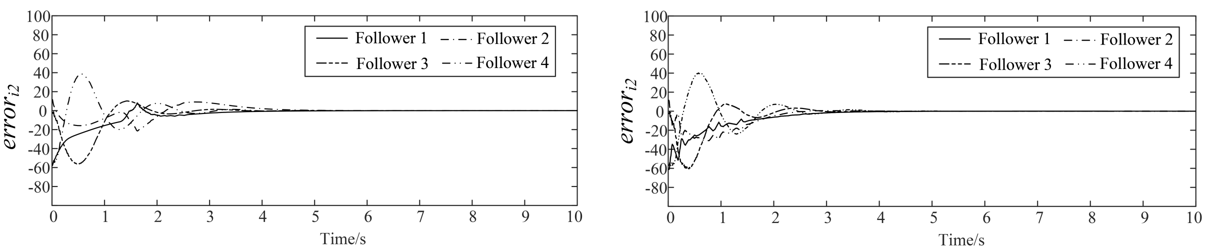

(a) (b)

FIGURE 6. $e_{i2}(t)$ between the observed and actual values: (a) Before improvement; (b) after improvement

6. **Conclusions.** This paper investigates the containment control problem in heterogeneous MAS within the context of switching topologies. A novel event-triggered variable coupling coefficient control strategy is proposed. The design includes a distributed dynamic feedback control scheme for followers, incorporating an event-triggered control mechanism to estimate the states of leaders. Furthermore, an effective coordination control rule

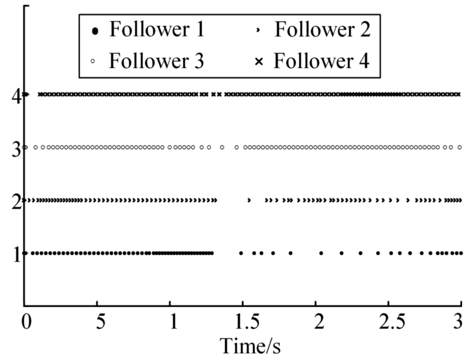

Figure 7. The event-triggered moments of the following agents

for variable coupling coefficients among multi-agents under switching topologies is introduced. This controller not only prevents collisions between agents but also accelerates the system's convergence, allowing the followers to converge faster more rapidly the convex hull formed by multiple leaders. Additionally, the control strategy significantly reduces the number of information transmissions among agents, thereby diminishing communication load and network energy consumption. Simulation results demonstrate that the proposed controller reduces the time for MAS to achieve containment by approximately 30%.

This paper investigates linear systems, yet the practicality of most systems lies in their nonlinearity. Therefore, the future research direction pertains to the extension of the proposed method to nonlinear systems. Furthermore, this paper employs a fixed event triggering threshold. In future studies, there is potential to optimize communication efficiency by dynamically setting the event triggering threshold based on the agent's state.

REFERENCES

[1] O. Qasem, M. Davari and W. Gao, Hybrid iteration ADP algorithm to solve cooperative, optimal output regulation problem for continuous-time, linear, multi-agent systems: Theory and application in islanded modern microgrids with IBRs, *IEEE Transactions on Industrial Electronics*, 2023.

[2] M. Y. Lu, J. Wu, X. S. Zhan and T. Han, Consensus of second-order heterogeneous multi-agent systems with and without input saturation, *ISA Transactions*, vol.126, pp.14-20, 2022.

[3] C. Z. Yuan and H. B. He, Cooperative output regulation of heterogeneous multi-agent systems with a leader of bounded inputs, *IET Control Theory & Applications*, vol.12, no.2, pp.233-242, 2018.

[4] X. W. Dong, Z. Ren and Y. S. Zhong, Time-varying formation tracking for second-order multi-agent systems subjected to switching topologies with application to quadrotor formation flying, *IEEE Transactions on Industrial Electronics*, vol.64, no.6, pp.5014-5024, 2017.

[5] X. W. Dong, Z. Ren and Y. S. Zhong, Theory and experiment on formation-containment control of multiple multirotor unmanned aerial vehicle systems, *IEEE Transactions on Automation Science and Engineering*, vol.15, no.1, pp.1-12, 2018.

[6] M. Patel and S. Datta, Control architecture for synchronization and tracking in descriptor multi-agent systems, *IEEE Control Systems Letters*, 2023.

[7] B. Wu and W. Liu, Event-triggered cooperative exponential practical tracking for a class of higher-order uncertain nonlinear multiagent systems, *IEEE Transactions on Systems, Man, and Cybernetics: Systems*, 2023.

[8] Y. Cao, Y. Luo, H. Yang and C. Luo, UAV-based emergency communications: An iterative two-stage multi-agent soft actor-critic approach for optimal association and dynamic deployment, *IEEE Internet of Things Journal*, 2023.

[9] W. Gan, X. Qu and D. Song, Multi-USV cooperative chasing strategy based on obstacles assistance and deep reinforcement learning, *IEEE Transactions on Automation Science and Engineering*, 2023.

[10] Y. Y. Ye, H. Y. Wei, R. Q. Lv and Y. Q. Wu, Containment control for networked fractional-order systems with sampled position data, *IEEE Transactions on Circuits and Systems I: Regular Papers*, vol.68, no.9, pp.3881-3889, 2021.

[11] Z. Li, J. Wu, X. Zhan et al., Distributed finite-time adaptive containment and bipartite containment control for nonlinear multi-agent system, *International Journal of Control, Automation and Systems*, vol.21, no.5, pp.1570-1580, 2023.
[12] Y. M. Hu, L. Chao and Z. M. Yuan, Distributed L_2-L_∞ containment control with nonconvex constraints for multi-agent systems, *Information Sciences*, vol.633, pp.1-9, 2023.
[13] Y. Li, J. H. Park, C. Hua and G. Liu, Distributed adaptive output feedback containment control for time-delay nonlinear multiagent systems, *Automatica*, vol.127, 2021.
[14] L. Mo, X. Yuan and Y. Yu, Containment control multi-agent systems with fractional Brownian motion, *Applied Mathematics and Computation*, vol.398, DOI: 10.1016/j.amc.2020.125814, 2021.
[15] J. Zhang, H. Zhang, Y. Cai and W. Li, Containment control of general linear multi-agent systems by event-triggered control mechanisms, *Neurocomputing*, vol.433, pp.263-274, 2021.
[16] L. Rong and Y. Hua, Distributed multi-agent containment control with event-triggered communications, *2018 37th Chinese Control Conference (CCC)*, pp.6711-6715, 2018.
[17] T. Xu, Y. Hao and Z. Duan, Fully distributed containment control for multiple Euler-Lagrange systems over directed graphs: An event-triggered approach, *IEEE Transactions on Circuits and Systems I: Regular Papers*, vol.67, no.6, pp.2078-2090, 2020.
[18] Q. Sun, X. Wang and Y.-H. Chen, Satellite formation-containment control emphasis on collision avoidance and uncertainty suppression, *IEEE Transactions on Cybernetics*, vol.53, no.8, pp.5121-5134, DOI: 10.1109/TCYB.2022.3173683, 2023.
[19] Y. Liu, P. Huang, F. Zhang and Y. Zhao, Distributed formation control using artificial potentials and neural network for constrained multiagent systems, *IEEE Transactions on Control Systems Technology*, vol.28, no.2, pp.697-704, 2020.
[20] Q. Deng, P. Yan, Q. Dong, H. Tao and X. S. Zhan, Neuro-adaptive containment control of unmanned surface vehicles with disturbance observer and collision-free, *ISA Transactions*, vol.129, pp.150-156, 2022.
[21] Q. Shi, T. Li, J. Li, C. P. Chen, Y. Xiao and Q. Shan, Adaptive leader-following formation control with collision avoidance for a class of second-order nonlinear multi-agent systems, *Neurocomputing*, vol.350, pp.282-290, 2019.
[22] L. Chen and H. B. Duan, Collision-free formation-containment control for a group of UAVs with unknown disturbances, *Aerospace Science and Technology*, vol.126, 2022.
[23] W. Zhao and F. L. Ren, Finite-time and fixed-time consensus for multi-agent systems via pinning control, *Applied Mathematics and Mechanics*, vol.42, no.3, pp.299-307, 2021.
[24] M. Firouzbahrami and A. Nobakhti, Cooperative fixed-time/finite-time distributed robust optimization of multi-agent systems, *Automatica*, vol.142, 2022.
[25] W. J. Wei and J. B. Yu, Global inverse optimal control for IT2 T-S fuzzy nonlinear multi-agent system under directed switching topologies, *Control Theory & Applications*, vol.39, no.10, pp.1985-1994, 2022.
[26] F. Y. Wang, H. Y. Yang, Z. X. Liu and Z. Q. Chen, Containment control of leader-following multi-agent systems with jointly-connected topologies and time-varying delays, *Neurocomputing*, vol.260, pp.341-348, 2017.
[27] W. H. Liu, C. J. Yang, Y. X. Sun and J. X. Qin, Observer-based event-triggered containment control of multi-agent systems with time delay, *International Journal of Systems Science*, vol.48, no.6, pp.1217-1225, 2017.
[28] Y. N. Sun, W. C. Zou, J. Guo and Z. R. Xiang, Containment control for heterogeneous nonlinear multi-agent systems under distributed event-triggered schemes, *Frontiers of Information Technology & Electronic Engineering*, vol.22, no.1, pp.107-119, 2021.
[29] H. Haghshenas, M. A. Badamchizadeh and M. Baradarannia, Containment control of heterogeneous linear multi-agent systems, *Automatica*, vol.54, pp.210-216, 2015.
[30] D. V. Dimarogonas, E. Frazzoli and K. H. Johansson, Distributed event-triggered control for multi-agent systems, *IEEE Transactions on Automatic Control*, vol.57, no.5, pp.1291-1297, 2012.

Author Biography

Wenchao Ma received his master's degree from Henan Polytechnic University in December 2015. He is currently working as the director of the Teaching and Research Section of Department of Locomotive and Vehicle Engineering, Zhengzhou University of Railway Engineering, and his research direction is electrical automation and automatic control. He has published 8 academic papers, one invention patent, one utility model patent, and presided over one provincial scientific research project. His research interests are related to automation control and its related application.